Available online at www.sciencedirect.com

ScienceDirect

Ceramics International 41 (2015) 3069–3074

CERAMICS INTERNATIONAL

www.elsevier.com/locate/ceramint

A theoretical investigation of the structural and electronic properties of orthorhombic $CaZrO_3$

I.L.V. Rosa[a], M.C. Oliveira[a,b], M. Assis[a], M. Ferrer[a], R.S. André[a], E. Longo[b], M.F.C. Gurgel[c,*]

[a]LIEC–Department of Chemistry, Universidade Federal de São Carlos, Via Washington Luiz, Km 235, P.O. Box 676, 13565-905 São Carlos, São Paulo, Brazil
[b]Institute of Chemistry, Universidade Estadual Paulista—Unesp, P.O. Box 355, 14801-907 Araraquara, São Paulo, Brazil
[c]Department of Chemistry, Universidade Federal de Goiás, Regional de Catalão, Av. Dr. Lamartine Pinto de Avelar, 75704-020 Catalão, Goiás, Brazil

Received 30 July 2014; received in revised form 21 October 2014; accepted 25 October 2014
Available online 6 November 2014

Abstract

A $CaZrO_3$ (CZO) powder was prepared by the soft chemical, polymeric precursor method (PPM). The CZO crystalline structure was investigated by powder X-ray diffraction (XDR), Retveld Refinament data, Raman spectra and ultraviolet–visible absorption spectroscopy. A theoretical study was performed using a periodic quantum mechanical calculation (CRYSTAL09 program). The periodic model built for the crystalline CZO structure was consistent with the experimental data obtained from structural and electronic properties. These results show that the material has an orthorhombic structure with experimental and theoretical gap values of 5.7 eV and 6.2 eV, respectively. In this article, we discuss the hybridization process of the oxygen p-orbitals and of the zirconium d-orbitals and analyze their band structures and density of states (partial and total).

Keywords: Perovskite; First principles; Electronic properties; CZO

1. Introduction

ABO_3 perovskites (where A = Ca, Sr, Pb or Ba and B = Ti or Zr) are oxides that have been extensively investigated due to their significance in fundamental research and in various technological applications [1–3]. These perovskite-type structures, where A and B are cations that correspond to oxygen ions, can have various symmetries (e.g. cubic unit cell, tetragon and distorted) depending on processing conditions and structural order [4]. Interest is increasing in these materials because of their physical and chemical properties that are optimal for diverse applications. Many studies have proposed low-cost preparation methods. The literature reports several synthesis methods such as a solid-state reaction [5], propionic acid routes [6], malate [7], co-precipitation [8], sol-gel [9], modified Pechini [10] and citrate [11].

Calcium Zirconate (CZO) has excellent chemical and physical properties including chemical stability [12–14]. $CaZrO_3$ is an orthorhombic perovskite (Pcnm space group) at ambient temperatures. This structure consists of small deformations in the ZrO6 octahedron with Zr-O bond lengths from 2.091(1) to 2.101(1) Å and O-Zr-O bond angles from 88:0(1)° to 99:0(1)°. $CaZrO_3$ can be cubic with Pbnm (at low temperature) and Pm3m (after high temperature heat treatment) space groups [15].

Brik et al. [16] used the DFT method to investigate the structural, electronic, and energy properties of the surface (0 0 1) of the CZO cubic terminations (CaO and ZrO). They observed that the CaO surface termination had lower energy and calculated 3.283 eV (LDA) and 3.315 eV (GGA) for the CZO cubic structure.

Hou [17] used the pseudopotential method for plane wave calculations to analyze the structural and electronic properties, and the elastic constant of the cubic CZO and concluded that the material is mechanically stable with a band gap of 3.30 eV.

Stoch et al. [18] showed that CZO obtained through a solid-state reaction has a similar orthorhombic structure. The full

*Corresponding author. Tel.: +55 64 34415334; fax: +5564 34415300.
E-mail address: mfcgurgel@hotmail.com (M.F.C. Gurgel).

http://dx.doi.org/10.1016/j.ceramint.2014.10.149
0272-8842/

potential linear plane wave method (FLAPW) showed the gap values of 4.1 eV.

Our group used periodic ab intio analysis to investigate correlations between experimental and theoretical studies on perovskites [19–24]. In the present study, we present XDR, UV–vis and Raman spectroscopy of crystalline orthorhombic CZO prepared by PPM. We built a periodic model based on Rietveld refinement data and associated the results with the quantum mechanical theoretical study to investigate the structure and electronic properties of this important material.

2. Experimental details

2.1. Synthesis of pure CZO

Pure CZO was obtained by dissolving $ZrOCl_2.8H_2O$ (0.0102 mol) into 40.0 mL of deionized water (60 °C) while stirring. Then, $C_6H_8O_7$(0.1224 mol) and $CaCl_2.2H_2O$ (0.0102 mol) were added. Next, ethyleneglycol was added and the temperature increased to 80 °C, promoting there actional polymerization. This process converted the material into a resin. The resin was then heated at 350 °C for 4 h causing pyrolysis. Finally, the material was heated again at 900 °C for 2 h, resulting in the crystallized CZO material [22].

2.2. Rietveld refinements and characterization

The CZO crystalline powder was analyzed by X-ray diffraction (XRD). The diffraction patterns of the crystalline powders were recorded by a Rigaku RINT2000 diffractometer in step scan mode (D2 h=0.02_, 20_ 6 2 h 6 130_) using copper radiation (kKa1=1.5406 A°, kKa2=1.5444 A°, Ka1/Ka2=0.5) monochromatized by a graphite crystal. The tube power was 42 kV · 120 mA, with a divergence slit of 0.5 mm and receiving slit of 0.30 mm. Rietveld refinements [25] were performed with the GSAS program [26]. The peak profile function was modeled using the Thompson-Cox-Hastings pseudo-Voigt (pV-TCH) convolution with the asymmetry function described by Finger et al. [27]. Strain anisotropy broadening was corrected by the phenomenological model described by Stephens [28]. Raman spectra were recorded on an RFS/ 100/S Bruker FT-Raman spectrometer with Nd:YAG laser providing excitation light (1064 nm), at a spectral resolution of 4 cm^{-1}. The UV–vis absorption spectra of the CZO powders were measured with a Cary 5 G instrument.

Table 1
Rietveld refinement data for pure CZO.

Space group=*Pnmc*			
Lattice parameter (Å)	a=5.59444	b=8.02115	c=5.76111
Centralatoms	Atomic coordinates		
	X	Y	Z
Calcium	0.0125	0.25	0.04798
Zirconium	0.0	0.0	0.5
Oxygen 1	0.61301	0.25	−0.04238
Oxygen 2	0.29986	0.05664	0.3011
Agreement indicies			
R_{wp} 8.02%	R_F^2 3.02%	χ^2 1.301	

2.3. CZO structure and periodic model details

Periodic quantum mechanical calculations (ab initio) were performed using the CRYSTAL09 [29] program and showed the orthorrombic structure with Pcnm space group of the CZO material. A package within the framework of the Density Functional Theory and a gradient-corrected correlation function by Lee, Yang and Parr, combined with the Becke3 exchange functional (B3LYP) were employed. The atomic centers were described by all-electron basis sets for the Ca, Zr, Ti and O atoms [30]. The XCrySDen program was used to design the periodic model and band structure and to outline the density of states diagrams [31]. We built the periodic model

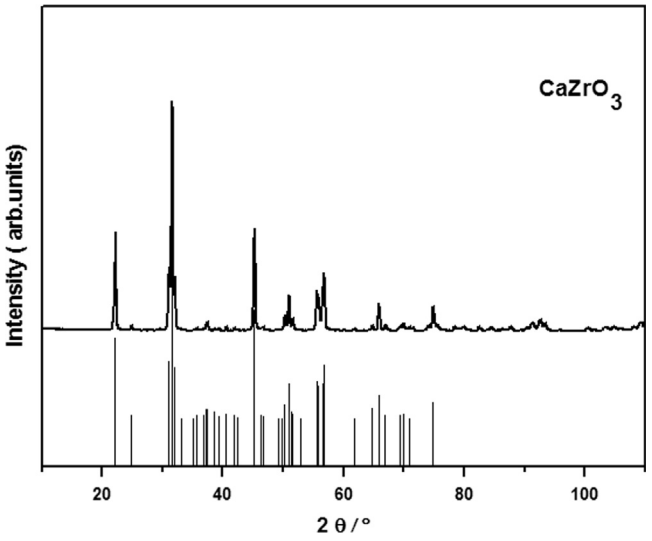

Fig. 1. XRD patterns for crystalline CZO powder annealed at 900 °C for 2 h.

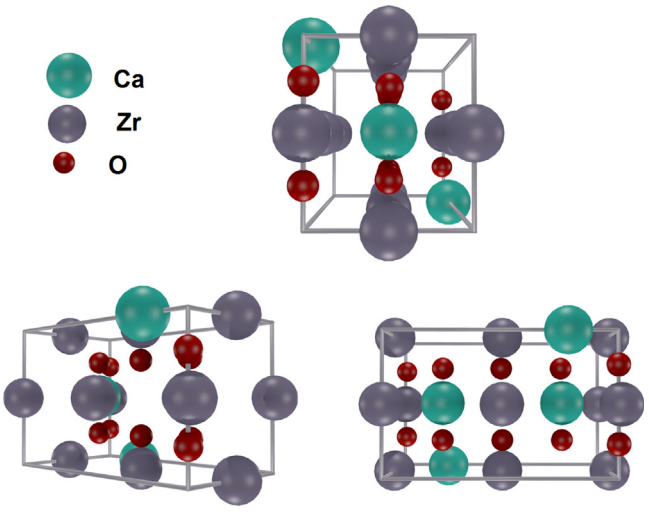

Fig. 2. Representation of the unit cell to periodic model CZO.

based on the Rietveld refinement results (Table 1) for the CZO crystalline structure of using a unit cell to represent the periodic models.

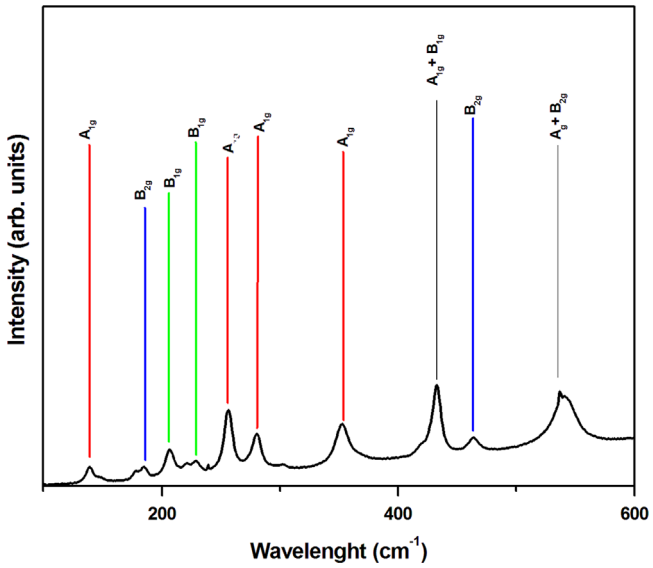

Fig. 3. Raman spectrum of the CZO material, heat-treated at 900 ° C for 2 h.

3. Results and discussion

3.1. X-ray diffraction

Fig. 1 illustrates the XRD patterns of the CZO powders calcined at 900 °C for 2 h. The pattern is typical of the ordered orthorhombic perovskite phase (n° 35–0790)

3.2. Rietveld refinement

The Rietveld refinement results (Table 1) were used to construct the periodic pattern of the CZO (Fig. 2). This periodic model consists of 4 zirconium atoms, 4 calcium atoms and 12 oxygen atoms, resulting in an orthorhombic structure (Pcmn).

3.3. Raman spectroscopy

Raman spectroscopy measurements were performed to identify the material at short range. Fig. 3 shows the Raman spectrum for the ceramic CZO powder annealed at 900 °C/ for 2 h.

Fig. 3 shows the Raman spectrum of CZO heat-treated at 900 °C for 2 h. This spectrum has peaks that are characteristic of a material with a short-range orthorhombic structure. The frequencies of the CZO Raman active modes (Table 2) are in

Table 2
Frequencies (cm^{-1}) of the Raman active modes for CZO powders heat-treated at 900 °C for 2 h.

Rights	CZO obtained (λ cm^{-1})	M. Tarrida, et al. [33] (Ca,Sr)ZrO_3 and Ca(Sn,Zr)O_3) (*Pnma*) symmetry group.	H. Zheng, et. al.[34] $CaZrO_3$–$CaTiO_3$ (*Pnma*) symmetry group.	V.M. Orera, et al. [35] $CaZrO_3$ (*Pcmn*) symmetry group.	P. McMillan, et al.[36] $CaZrO_3$ *(Pbnm)* symmetry group.	C.H. Perry, et al.[37] $CaZrO_3$ Orthorhombic
(A_g) Network modes (Ca-ZrO_3)	141			145	143	
		151				153
		172				
(B_{2g}) bonding modes (flexion) (O-Zr-O)	185	185			182	186
		193	190	190	189	
(B_{1g}) bonding modes (flexion) (O-Zr-O)	206	213	212	212	212	
(B_{1g}) bonding modes (flexion) (O-Zr-O)	228	229	227	227	224	228
		235	233	234	233	
(A_g) bonding modes (flexion) (O-Zr-O)	257	263	262	262,5	260	
(A_g) bonding modes (flexion) (O-Zr-O)	281	287	286	286,5	285	
				305	302	
					338	340
(A_g) torsional modes (Zr-O_3)	354	358	357	358	356	
					370	377
					408	
(A_g +B_{1g}) torsional modes (Zr-O_3)	433	423	437	418	423	418
		439	439	439	437	
(B_{2g}) stretching modes	464	470		469	468	515
(A_g +B_{2g}) stretching modes	537		543	543		
		548		547	545	551

agreement with the literature [32–37]. The overall half-width at half-height of the Raman spectrum bands is proportional to the inverse of the grain size. The frequencies at 141 cm^{-1} and 185 cm^{-1} correspond to the A_{1g} vibrational modes and the Zr-O (B_{2g}) bending modes, respectively. The frequencies at 206 and 228 cm^{-1} are ascribed to the Zr -O bending modes (B_{1g}). The 257 and 281 cm^{-1} frequencies are ascribed to the Zr -O bending (A_{1g}) modes, 354 cm^{-1} to the torsional mode (A_{1g}) and 433 cm^{-1} to the torsional modes ($A_{1g}+B_{1g}$). The Raman band at the stretching modes Zr-O ($A_{1g}+B_{2g}$) is also apparent.

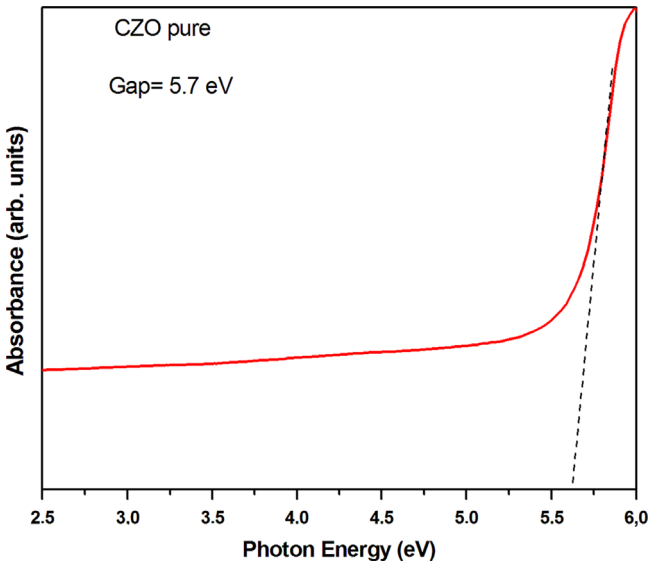

Fig. 4. Absorption Spectrum as a function of energy (eV) for the CZO powder heat-treated at 900 °C for 2 h.

3.4. UV–vis spectroscopy

Fig. 4 shows the optical absorption curve as a function of photon energy for the pure CZO samples.

The experimental E_{gap} value for this sample was calculated by the Wood and Tauc method, which relates sample absorbance with photon energy to obtain the optical energy gap (E_{gap}) [38].

The UV–vis absorbance spectrum (Fig. 4) shows that the Gap Energy is 5.7 eV. This experimental gap value is in good agreement with the theoretical Egap of 6.23 eV.

3.5. Band structure

K-point sampling was conducted at 40 points within the irreducible part of the Brillouin zone. The theoretical results were represented in terms of band structures. Fig. 5(a-c) illustrate the Brillouin zone, band structure and atomic orbital contributions related to the oxygen, zirconium and calcium atoms. Fig. 5(a) illustrates that the Brillouin zone for the unit cell is determined by the CZO kpoints: Γ́=(0,0,0), X=(1/2,0,0) Z=(1/2,0,0); U=(0,0,1/2); T=(0,1/2,1/2), Γ́=(0,0,0). The gap was evaluated as 6.23 eV, which is considered a direct gap from (0,0,0) to (0,0,0) kpoints. Fig.5(b) represents the structure band. Fig. 5(c) shows the valence band (VB) from 0 to -0.62 eV where the oxygen orbitals (px, py and pz) are located. Fig. 5(d) shows the conduction band (CV) of the zirconium atomic orbitals $4d_z^2$, $4d_{xy}^2$, $4d_{xy}$, $4d_{xz}$, $4d_{yz}$, situated from 6.23 to 8.11 eV. Slight contributions from the atomic orbitals of the Ca atoms are also visible.

Several researchers have used computational methods and theoretical models to interpret the structural and electronic properties of calcium zirconate with cubic and orthorhombic structures [16–18]. Our article discusses an experimental and

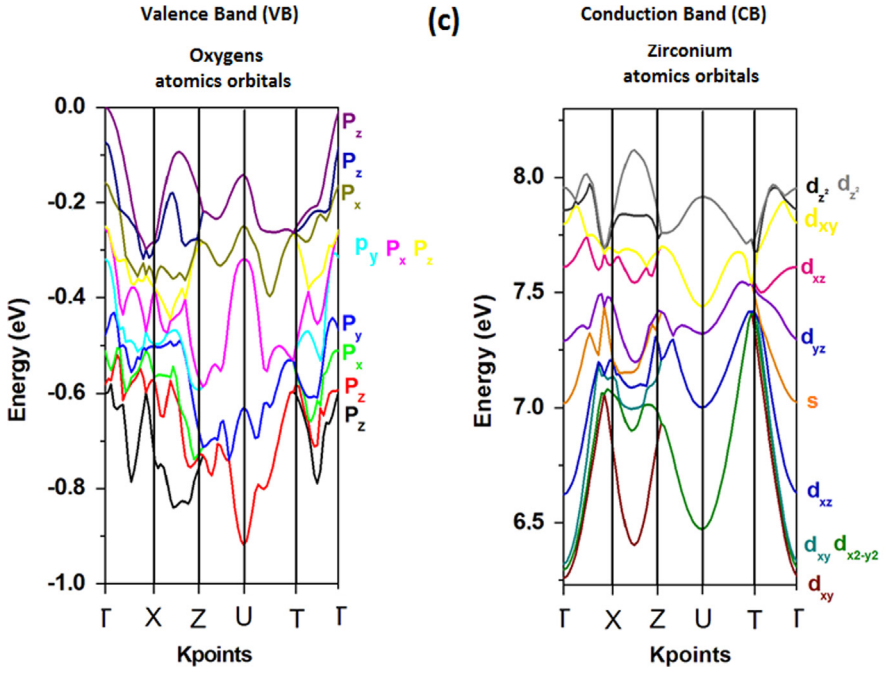

Fig. 5. Representation of the CZO band structure (a) brillouin zone, (b) band structure, (c) p atomic orbitals in the VB and (d) d and s atomic orbitals in the CB.

theoretical study of orthorhombic CZO. We synthesized the material by PPM and carried out computations using the CRYSTAL 09 program [29]. In the case of CZO synthesized by the MPP procedure both experimental and theoretical Egap values are 5.7 and 6.23 eV, respectively

3.6. Partial DOS

Fig. 6(a-d) shows total DOS of CZO from the atomic orbitals of zirconium, calcium and oxygen, respectively. Some of the atoms in this structure contribute equally given the structural symmetry of CZO. A predominant contribution of d and p atomic orbitals from the Zirconium and Oxygen atoms in the conduction band region (CB) and in the valence band region (BV), respectively, was noticed. The s contributions of the atomic orbitals from the Calcium atoms are also present in the CB and BV bands being, however, less intense. Fig. 6(a) illustrates the equivalent contributions to total DOS from the atomic orbitals (4d) of the four zirconium atoms (Zr_{1-4}). Fig. 6 (b) shows the equivalent contributions from the atomic orbitals of the four calcium atoms (Ca_{1-4}). The CZO structure is composed of twelve oxygen atoms with contributions from the px, py and pz orbitals. DOS from the oxygen atoms was divided into two equivalent oxygen groups (O_{1-4} and O_{5-12}) (Fig. 6c-d).

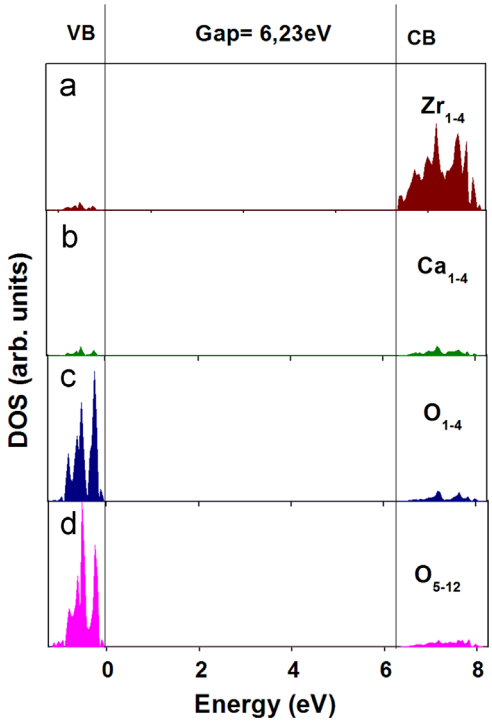

Fig. 6. Total DOS from the pure CZO: (a) 4 zirconium atoms (Zr1-4) (b) 4 calcium atoms (Ca1-4), (c) 4 oxygen atoms (O1-4) and (d) 8 oxygen atoms (O5-12).

Fig. 7(a) shows the CZO unit cell and the diagonal plane designated by the red dots among the Zr-O-Ca-O-Zr atoms. Fig. 7(b) illustrates the electron density map of the Ca, Zr and O atoms and shows contour lines indicating hybridization among the atoms in the diagonal plane. A homogeneous borderline between the Zr-O and Ca-O atoms representing covalent and ionic bonds, respectively [39].

4. Conclusions

Crystalline CZO was synthesized by PPM. XRD patterns, Rietveld refinement and Raman spectroscopy confirmed the orthorhombic structure of this material, whereas UVvis absorption allowed calculation of the value gap E_{gap} (5.7 eV). The periodic quantum mechanical calculation (PQMC) through CRYSTAL09 was used to determine the first-principle calculations needed to study the structure and electronic properties of CZO. Our theoretical band structure and DOS results show hybridization between Zr and O atoms resulting from strong covalent bonding between zirconium d-states of and oxygen p-states. CZO has a direct band gap with $E_{gap}=6.23$ eV.

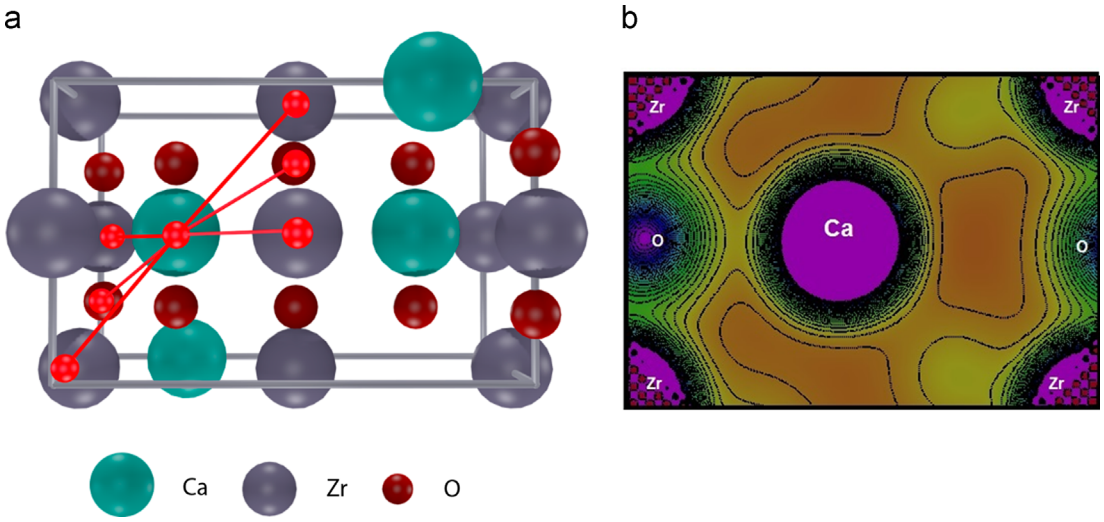

Fig. 7. Representation of the Zr-Ca-O diagonal plane from CZO (a) unit cell and (b) electron density map.

Acknowledgments

The financial support of this research project by the Brazilian research funding agencies CNPq, CAPES and FAPESP is gratefully acknowledged

References

[1] V.V. Bannikov, I.R. Shein, V.L. Kozhevnikov, A.L. Ivanovskii, Magnetism without magnetic ions in non-magnetic perovskites SrTiO3, $SrZrO_3$ and $SrSnO_3$, J. Magn. Magn. Mater. 320 (2008) 936–942.

[2] M.F.C. Gurgel, M.L. Moreira, E.C. Paris, J.W.M. Espinosa, P.S. Pizani, J.A. Varela, E. Longo, $BaZrO_3$ photoluminescence property: an Ab initio analysis of structural deformation and symmetry changes, Int. J. Quantum Chem. 111 (2011) 694–701.

[3] H. Pinto, A. Stashans, Computational study of self-trapped hole polarons in tetragonal BaTiO3, Phys. Rev. B 65 (2002) 1343041–1343046.

[4] P.S. Pizani, E.R. Leite, F.M. Pontes, E.C. Paris, J.H. Rangel, E.J.H. Lee, E. Longo, P. Delega, J.A. Varela, Photoluminescence of disordered ABO (3) perovskites, Appl. Phys. Lett. 77 (2000) 824–826.

[5] K.R. Kambale, A.R. Kulkarni, N. Venkataramani, Grain growth kinetics of barium titanate synthesized using conventional solid state reaction route, Ceram. Int. 40 (2014) 667–673.

[6] T. Horikawa, N. Mikami, T. Makita, J. Tanimura, M. Kataoka, K. Sato, M. Nunoshita, Dielectric-properties of $(Ba,Sr)TiO_3$ thin-films deposited by rf-sputtering, Jpn. J. Appl. Phys. 1 (32) (1993) 4126–4130.

[7] C. Marcilly, P. Courty, B. Delmon, Preparation of highly dispersed mixed oxides and oxide solid solutions by pyrolysis of amorphous organic precursors, J. Am. Ceram. Soc. 53 (1970) 56–57.

[8] A.V. Murugan, V. Samuel, S.C. Navale, V. Ravi, Phase evolution of $NiTiO_3$ prepared by coprecipitation method, Mater. Lett. 60 (2006) 1791–1792.

[9] I. Chilibon, J.N. Marat-Mendes, Ferroelectric ceramics by sol-gel methods and applications: a review, J. Sol-Gel Sci.Techol. 64 (2012) 571–611.

[10] Y.J. Lin, Y.H. Chang, W.D. Yang, B.S. Tsai, Synthesis and characterization of ilmenite $NiTiO_3$ and $CoTiO_3$ prepared by a modified Pechini method, J. Non-Cryst. Sol. 352 (2006) 789–794.

[11] H. Taguchi, D. Matsuda, M. Nagao, K. Tanihata, Y. Miyamoto, Synthesis of perovskite-type $(La_{1-X}Sr_x)MnO_3$ (O-less-than-or-equal-to-X-less-than-or-equal-to-0.3) at low-temperature, J. Am. Ceram. Soc. 75 (1992) 201–202.

[12] Y. Du, Z.P. Jin, P.Y. Huang, Thermodynamic calculation of the zirconia calcia system, J. Am. Ceram. Soc. 75 (1992) 3040–3048.

[13] G. Rog, M. Dudek, A. Kozlowska-Rog, M. Bucko, Calcium zirconate: preparation, solid oxide properties and application to the galvanic cells, Electrochim. Acta 47 (2002) 4523–4529.

[14] J. Szczerba, Z. Pedzich, The effect of natural dolomite admixtures on calcium zirconate-periclase materials microstructure evolution, Ceram. Int. 36 (2010) 535–547.

[15] H.J.A. Koopmans, G.M.H. Vandevelde, P.J. Gellings, Powder neutron-diffraction study of the perovskites $CaTiO_3$ and $CaZrO_3$, Acta Crystallogr. C 39 (1983) 1323–1325.

[16] M.G. Brik, C.G. Ma, V. Krasnenko, First-principles calculations of the structural and electronic properties of the cubic $CaZrO_3$ (001) surfaces, Surf. Sci. 608 (2013) 146–153.

[17] Z.F. Hou, Ab initio calculations of elastic modulus and electronic structures of cubic $CaZrO_3$, Phys. B –Condens. Matter 403 (2008) 2624–2628.

[18] P. Stoch, J. Szczerba, J. Lis, D. Madej, Z. Pedzich, Crystal structure and ab initio calculations of $CaZrO_3$, J. Am. Ceram. Soc 32 (2012) 665–670.

[19] M.S.C. Camara, M.F.C. Gurgel, S.R. Lazaro, T.M. Boschi, P.S. Pizani, E.R. Leite, A. Beltran, E. Longo, Room temperature photoluminescence of the $Li_2ZnTi_3O_8$ spinel: Experimental and theoretical study, Int. J. Quantum Chem. 103 (2005) 580–587.

[20] L.S. Cavalcante, N.C. Batista, T. Badapanda, M.G.S. Costa, M.S. Li, W. Avansi, V.R. Mastelaro, E. Longo, J.W.M. Espinosa, M.F.C. Gurgel, Local electronic structure, optical bandgap and photoluminescence (PL) properties of $Ba(Zr_{0.75}Ti_{0.25})O_3$ powders, Mater. Sci. Semicon. Proc. 16 (2013) 1035–1045.

[21] V.M. Longo, A.T. de Figueiredo, S. de Lazaro, M.F. Gurgel, M.G.S. Costa, C.O. Paiva-Santos, J.A. Varela, E. Longo, V.R. Mastelaro, F.S. De Vicente, A.C. Hernandes, R.W.A. Franco, Structural conditions that leads to photoluminescence emission in $SrTiO_3$: An experimental and theoretical approach, J. Appl. Phys. 104 (2008) 0235151–02351511.

[22] J.M.A. Nunes, J.W.M. Espinosa, M.F.C. Gurgel, P.S. Pizani, S.H. Leal, M. Santos, E. Longo, Photoluminescent properties of lead zirconate powders obtained by the polymeric precursor method, Ceram. Int. 38 (2012) 4593–4599.

[23] E.C. Paris, M.F.C. Gurgel, M.R. Joya, G.P. Casali, C.O. Paiva-Santos, T.M. Boschi, P.S. Pizani, J.A. Varela, E. Longo, Structural deformation monitored by vibrational properties and orbital modeling in $(Pb,Sm)TiO_3$ systems, J. Phys. Chem. Solids 71 (2010) 12–17.

[24] J.R. Sambrano, E. Orhan, M.F.C. Gurgel, A.B. Campos, M.S. Goes, C.O. Paiva-Santos, J.A. Varela, E. Longo, Theoretical analysis of the structural deformation in Mn-doped $BaTiO_3$, Chem. Phys. Lett. 402 (2005) 491–496.

[25] H.M. Rietveld, A profile refinement method for nuclear and magnetic structures, J. Appl. Crystallogr 2 (1969) 65.

[26] A.C. Larson, R.B. Von Dreele, General Structure Analysis System (GSAS) Program, Rep. N° (LAUR 86–748), Los Alamos National Laboratory, University of California, Los Alamos, NM, 2004.

[27] L.W. Finger, D.E. Cox, A.P. Jephcoat, A correction for powder diffraction peak asymmetry due to axial divergence, J. Appl. Crystallogr 27 (1994) 892–900.

[28] P.W. Stephens, Phenomenological model of anisotropic peak broadening in powder diffraction, J. Appl. Crystallogr. 32 (1999) 281–289.

[29] R. Dovesi, V.R. Saunders, C. Roetti, R. Orlando, C.M. Zicovich-Wilson, F. Pascale, B. Civalleri, K. Doll, N.M. Harrison, I.J. Bush, P.D.' Arco, M. Llunell, CRYSTAL09 User's Manual, University of Torino, Torino, 2009.

[30] CRYSTAL Basis Sets Library. ⟨http://www.crystal.unito.it/Basis_Sets/Ptable.html⟩, 2014 (accessed 04.07.14).

[31] A. Kokalj, XCrySDen - a new program for displaying crystalline structures and electron densities, J. Mol.Graph. Model. 17 (1999) 176–179.

[32] I. Levin, E. Cockayne, M.W. Lufaso, J.C. Woicik, J.E. Maslar, Local structures and Raman spectra in the $Ca(Zr,Ti)O_3$ perovskite solid solutions, Chem. Mater. 18 (2006) 854–860.

[33] P. McMillan, N. Ross, The raman-spectra of several orthorhombic calcium-oxide perovskites, Phys. Chem. Miner. 16 (1988) 21–28.

[34] V.M. Orera, C. Pecharroman, J.I. Pena, R.I. Merino, C.J. Serna, Vibrational spectroscopy of $CaZrO_3$ single crystals, J. Phys.-Condens. Matter 10 (1998) 7501–7510.

[35] C.H. Perry, D.J. McCarthy, G. Rupprech, Dielectric dispersion of some perovskite zirconates, Phys. Rev. 138 (1965) 1537–1538.

[36] M. Tarrida, H. Larguem, M. Madon, Structural investigations of (Ca,Sr) ZrO_3 and $Ca(Sn,Zr)O_3$ perovskite compounds, Phys. Chem. Miner. 36 (2009) 403–413.

[37] H. Zheng, I.M. Reaney, G. de Gyorgyfalva, R. Ubic, J. Yarwood, M.P. Seabra, V.M. Ferreira Raman, spectroscopy of $CaTiO_3$-based perovskite solid solutions, J. Mater. Res. 19 (2004) 488–495.

[38] D.L. Wood, J. Tauc, Weak absorption tails in amorphous semiconductors, Phys. Rev. B 5 (1972) 3144.

[39] D.F. Shriver, P.W. Atkins, Inorganic Chemistry, fourth ed., Oxford University, United States, 2006.